Supplementary Information

Thermally activated sensitization of organics by lanthanide complexes for near-infrared photochemical upconversion

Ling Zhang[a,c], Guohua Zhu[a,c], Rui Hu[b], Guoqiang Yang[b,c], Tianjun Yu[a], Jinping Chen[a], Yi Li[a,c], Yi Zeng[a,c*]

[a]Key Laboratory of Photochemical Conversion and Optoelectronic Materials, Technical Institute of Physics and Chemistry, Chinese Academy of Sciences, Beijing 100190, China. E-mail: zengyi@mail.ipc.ac.cn

[b]Key Laboratory of Photochemistry, Institute of Chemistry, Chinese Academy of Sciences, Beijing 100190, China.

[c]University of Chinese Academy of Sciences, Beijing 100049, China.

Experimental Method

General Experimental Details. General reagents were purchased from Beijing Innochem and used without further purification unless otherwise noted. 9,10-bis((triisopropylsilyl)ethynyl) anthracene (TIPS) was purchased from sigma-aldrich without extra purification. 9,10-Bis(phenylethynyl) anthracene (BPEA) was purchased from Energy Chemical and purified by recrystallization in toluene before use. N,N′-Bis(ethylpropyl)perylene-3,4,9,10-tetracarboxylicdimide (PDI) was purchased from a Bide Pharmatech Co., Ltd without extra purification. The liquid samples for UC measurement were prepared in a glove box, with O_2 concentration <0.1 ppm, and H_2O concentration <0.2 ppm. The solid samples for UC measurement were sealed between quartz coverslips with epoxy glue (Ergo 7300) in a glovebox (O_2 concentration <0.1 ppm).

Instrumentation. A suitable crystal was selected and on a XtaLAB AFC10 (RCD3): fixed-chi single diffractometer. The crystal was kept at 170 K during data collection. Using Olex2[1], the structure was solved with the SHELXT[2] structure solution program using Intrinsic Phasing and refined with the SHELXL[2] refinement package using Least Squares minimization. UV-vis absorption spectrum in the visible region and NIR region was recorded by using a Shimadzu UV-2550PC spectrophotometer and Agilent Cary 7000 spectrophotometer respectively. Visible emission spectra and NIR emission spectra were measured on Hitachi F-4600 spectrometer and Edinburgh FLS1000 spectrometer. The fluorescence lifetimes of the microcrystals were also recorded on an

Edinburgh FLS1000 spectrometer by a pulsed laser diode at 980 nm. FT-IR spectra were recorded with an Excalibur 3100 FT-IR spectrometer by incorporation of samples into KBr disks. Powder X-ray diffraction (PXRD) patterns were measured at a scanning rate of 5° min^{-1} in the 2θ range from 5 to 50° with a Bruker D8 Focus X-ray diffractometer equipped with Cu Kα radiation (λ = 1.54056 Å). SEM images were obtained using the Regulus 8230 cast on conductive adhesive substrates. An Edinburgh FLS1000 spectrometer was employed for temperature-dependent emission spectra. Experiments with temperature changing from 223 K to 293 K. All upconversion steady-state spectra were measured using Edinburgh FLS1000 spectrometer with an external continuous wave 980 nm laser diode (MRL-III-980, Changchun New Industries Optoelectronics Technology Co., Ltd.).

Determination of Thermal Sensitivity. The relative thermal sensitivity (Sr) in the unit of K^{-1} was determined according to $Sr = d_y/d_T/y \times 100\%$, where y and T were the ratio of dual emission peak intensity and temperature, respectively.

Synthesis and Characterization of the $Yb_5(DBM)_{10}(H_2O)_5$

Yb complex was synthesized according to the modified method[3, 4 5], described as follows:

A mixture of dibenzoylmethane (DBM) (2 mmol), and 1ml NaOH (1M) in 10 mL of ethanol was refluxed at 75℃ for 30 min. and then the 7 mL of $YbCl_3$.$6H_2O$ (1.00 mmol) water solution was slowly added in the mixture under stirring. After being refluxed for 3.5 h, a yellow precipitate formed. The suspension was allowed to cool to ambient temperature under stirring, the precipitate was collected on a Büchner funnel and washed with a minimum of ice-cold ethanol (ca. 10 mL). It was filtered and recrystallized from 20 mL of $CHCl_3$, crystallization upon cooling to 25°C. After drying the solid under reduced pressure for 5 h, the product $Yb_5(DBM)_{10}(OH)_5$ was obtained. (Mp. 255-265 ℃).

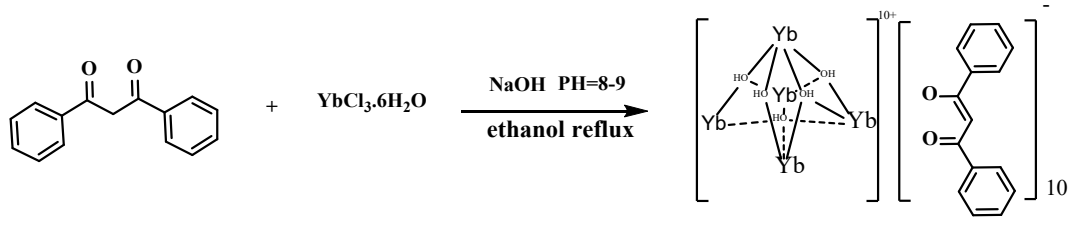

Scheme S1 Synthesis route of $Yb_5(DBM)_{10}(OH)_5$

Preparation signal crystal. A yellow tetragonal crystal suitable for single-crystal X-ray diffraction was obtained by the liquid-phase diffusion method. In a 5mL glass vial, 5 mg of $Yb_5(DBM)_{10}(OH)_5$ was dissolved in 2 mL of chloroform. The vial was then placed in a 20 mL glass vial containing 10

mL of cyclohexane. The outer glass bottle was sealed with a sealing film and left undisturbed at room temperature for one week.

Preparation of Microcrystals

Signal microcrystal. 10 mg annihilator was dissolved in 1 mL THF, and Yb-complexes in different molar proportions (1:10, 1:30, and 1:50, 1:100, respectively) were added to the solution. Then the solution of Yb-complex/annihilator was rapidly injected into 5 mL water at room temperature under 1000 rpm stirring for 2 min. The mixture stood for 2 h, and the doped microcrystal was collected by centrifugation at 8000 rpm for 5 min. Drying in vacuum ovens for 4h. The dry upconversion microcrystals are sealed between two coverslips in a glove box before testing. The annihilators are TIPS, BPEA and PDI, respectively.

Mixed microcrystal. 5 mg Yb-BPEA microcrystal and 50 mg Yb-PDI microcrystal were mixed by physical method. Yb-BPEA microcrystal and Yb-PDI microcrystal were placed in an oscillator shaken for 10 min to mix uniformity fully. The mixed microcrystal was placed in a glove box sealed between two coverslips before testing.

Preparation and Measurement of TTA-UC in Solution

In an argon atmosphere glovebox, the DMF solutions of Yb5(DBM)10(OH)5 (0.3 M), BPEA (4 mM), TIPS (2 mM), and PDI (2 mM) were prepared. The sensitizer and annihilator were mixed in varying proportions to create the TTA-UC system in the glove box. The prepared TTA-UC solution under argon was sealed into quartz cuvettes with a rubber stopper, and the upconversion spectra were obtained using an Edinburgh FLS1000 spectrometer equipped with a CW laser diode (980 nm).

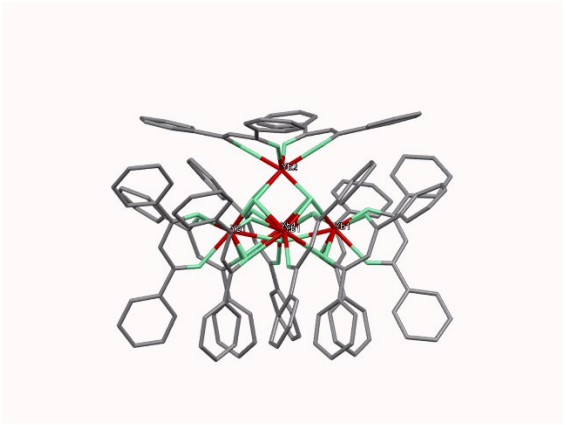

Fig. S1 Single-crystal XRD structure of $Yb_5(DBM)_{10}(OH)_5$ complex. Hydrogens have been omitted for clarity.

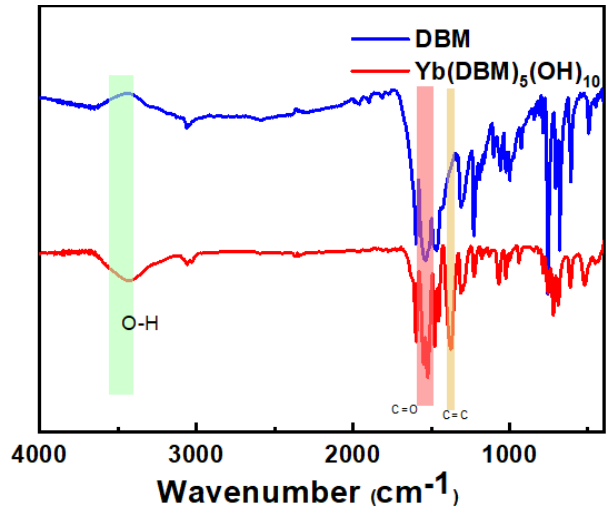

Fig. S2 FTIR spectra of $Yb_5(DBM)_{10}(OH)_5$ and DBM ligand.

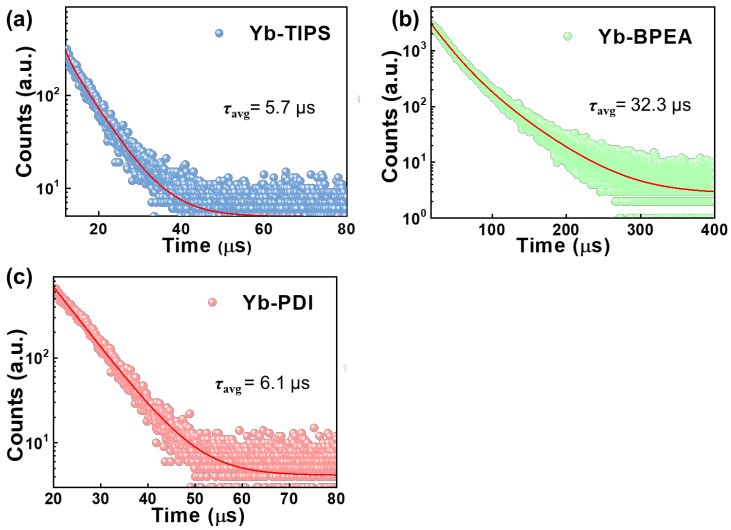

Fig. S3 The delayed fluorescence decay and tail-fitting curves of solid microcrystals Yb-TIPS (1:1) at 500nm (a), Yb-BPEA (1:30) at 560 nm (b), Yb-PDI (1:10) at 650 nm (c) (λ_{ex} = 980 nm with a CW laser diode).

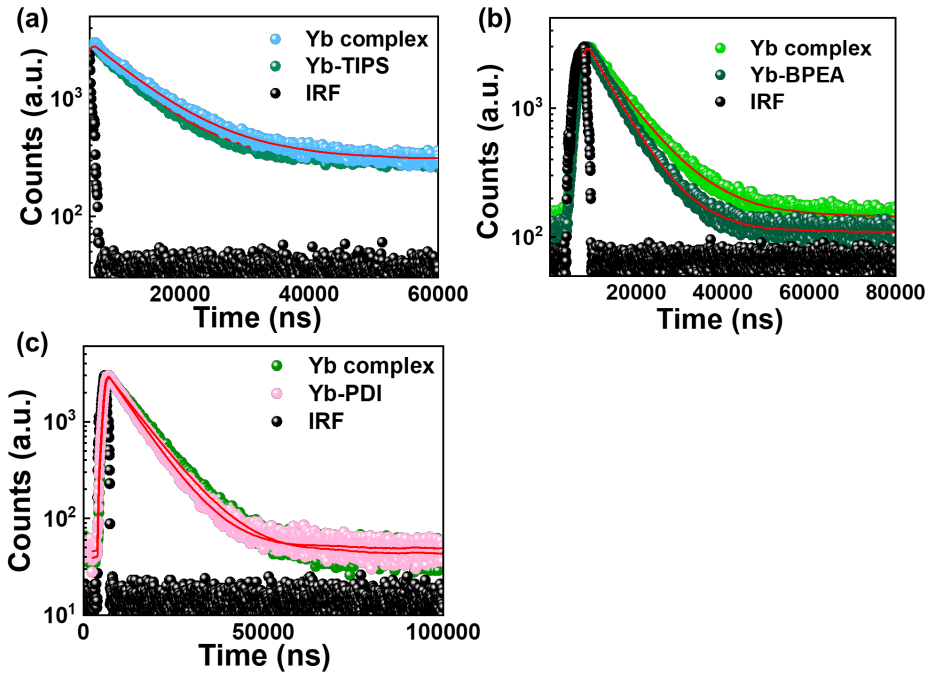

Fig. S4 Time-resolved decay curves of photosensitizer $Yb_5(DBM)_{10}(OH)_5$ and TTA-UC system of Yb-TIPS (6:1), Yb-BPEA (18:1), Yb-PDI (18:1) at 1010 nm in DMF (λ_{ex} = 980 nm).

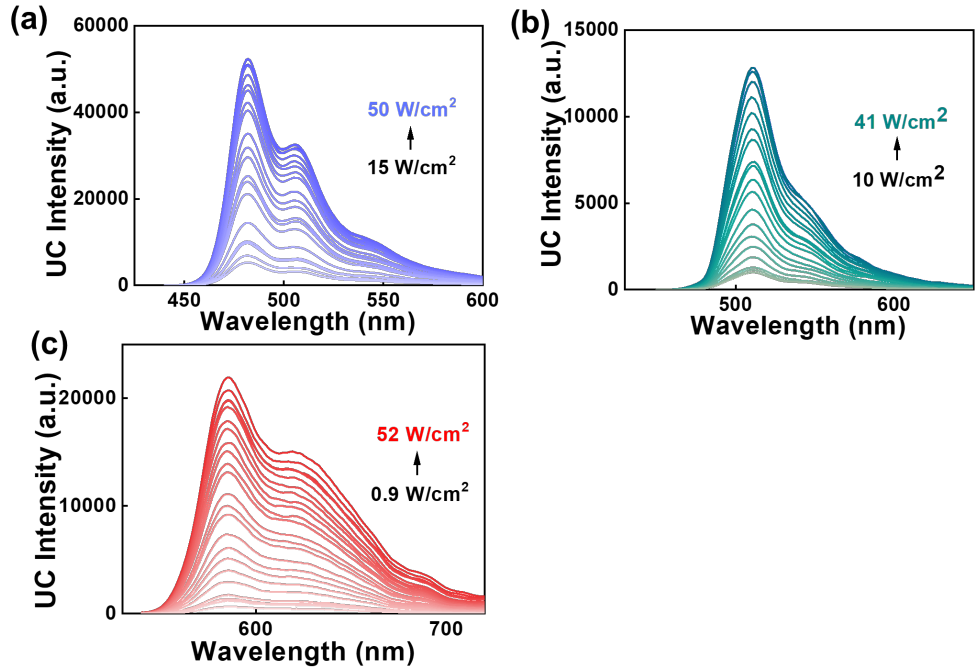

Fig. S5 UC emission spectra of Yb-TIPS (6:1) (a), Yb-BPEA (9:1) (b), Yb- PDI (36:1) (c) with various excitation in DMF (λ_{ex} = 980 nm).

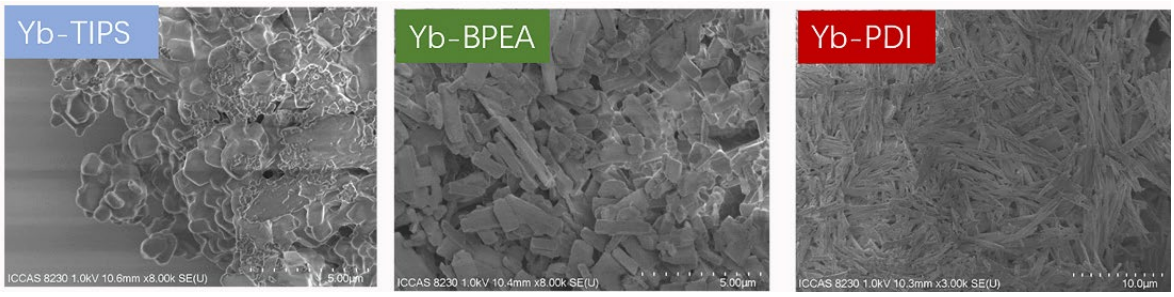

Fig. S6 The SEM of Yb-TIPS (1:1), Yb-BPEA (1:30), Yb-PDI (1:10) microcrystals.

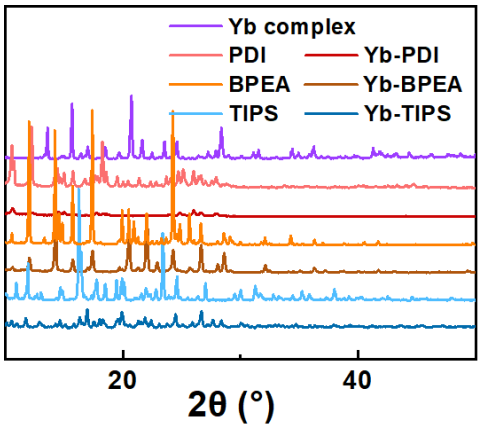

Fig. S7 The PXRD of PDI, Yb-PDI (1:10), BPEA, Yb-BPEA (1:30), TIPS and Yb-TIPS (1:1) microcrystals.

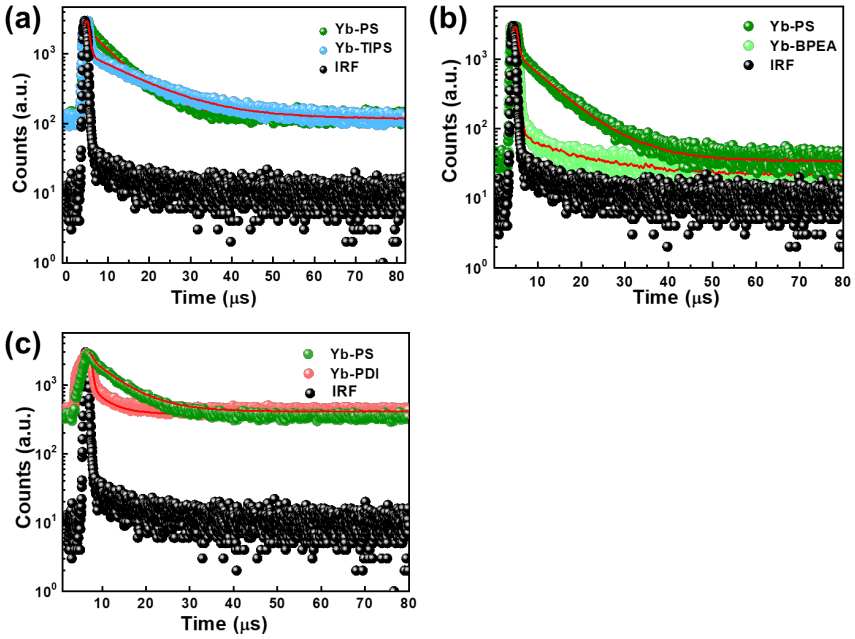

Fig. S8 Time-resolved emission of Yb5(DBM)10(OH)5 in polystyrene (PS) film and in Yb-TIPS (1:1), Yb-BPEA (1:30), Yb-PDI (1:10) microcrystals, respectively (λ_{ex} = 980 nm).

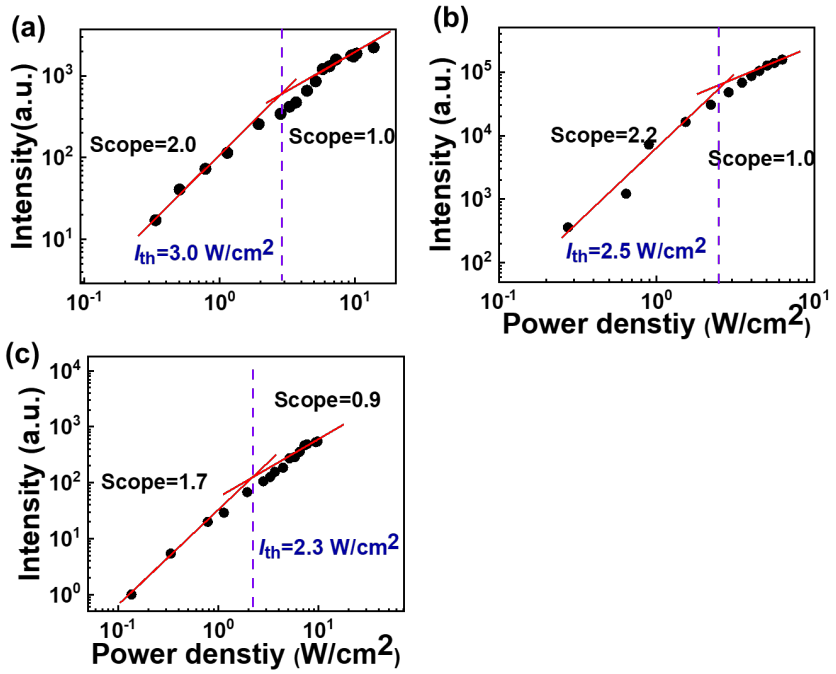

Fig. S9 Dependence of the TTA-UC intensity on the incident power densities of microcrystals: (a) Yb-TIPS (1:1), (b) Yb-BPEA (1:30), (c) Yb- PDI (1:10) (λ_{ex} = 980 nm with a CW laser diode).

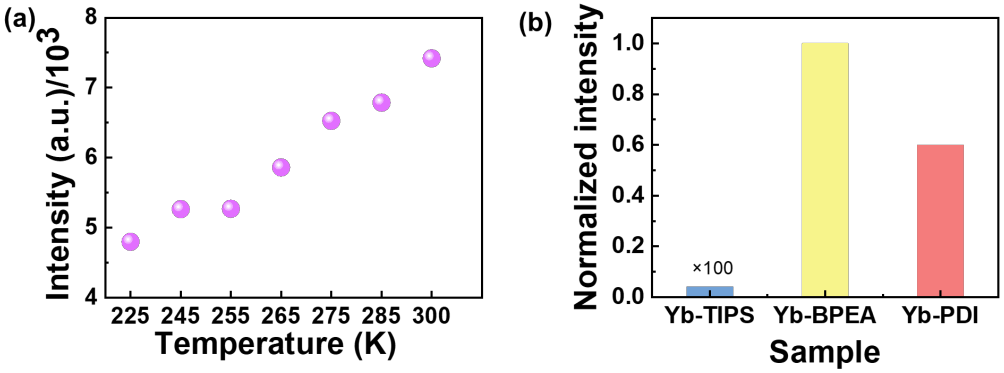

Fig. S10 The peak emission intensity of the solid Yb complex-doped TIPS microcrystal (molar ratio = 1:1) at various temperatures excited at 980 nm from 223 to 300 K (a) and the relative peak intensity of Yb-TIPS, Yb-BPEA and Yb-PDI excited at same power density (b).

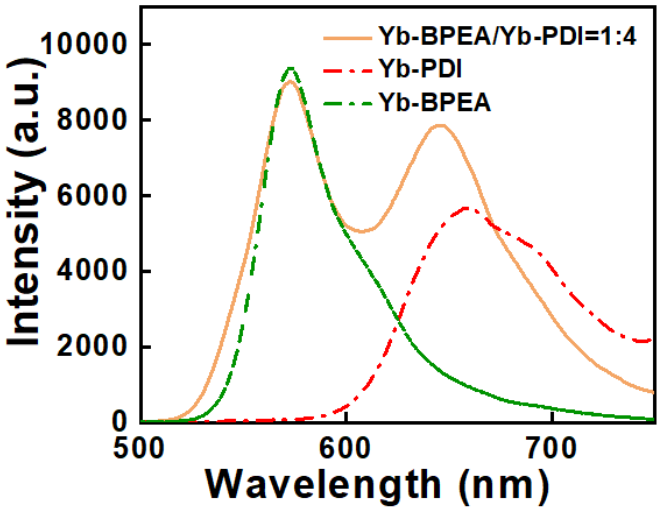

Fig. S11 UC emission spectra of the mixed microcrystals (orange), Yb-BPEA (green, 1:30) and Yb-PDI (red,1:10). The mixed microcrystal containing Yb-BPEA microcrystal (1:30) and Yb-PDI crystal (1:10). The mass ratio of Yb-BPEA /Yb-PDI is 1:4.

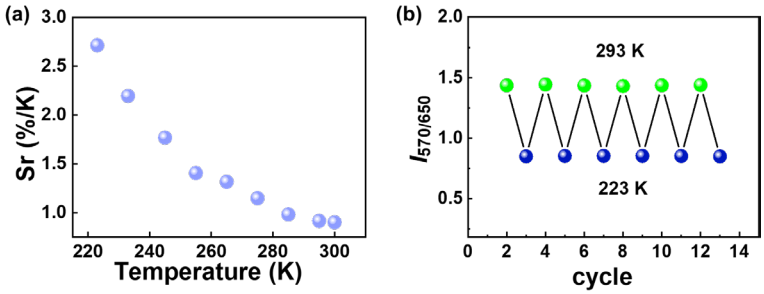

Fig. S12 The relative thermal sensitivity (a) and the reversibility of ratiometric upconversion emission (b) of microcrystal Yb-BPEA/Yb-PDI (1:4 w/w) from 223 to 293 K (λ_{ex} = 980 nm).

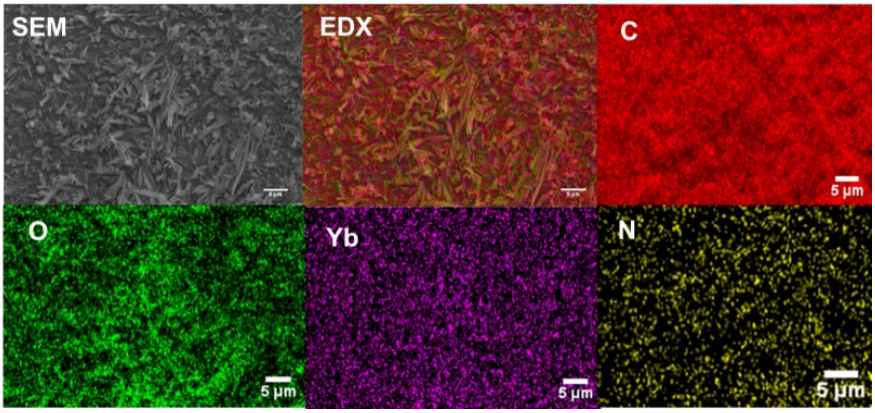

Fig. S13 The SEM and EDX-mapping image of mixed TTA-UC microcrystal (Yb-BPEA/Yb-PDI (1:4 w/w)) and the elemental mapping of C, O, N and Yb. The chemical composition of the mixed TTA-UC microcrystal of (Yb-BPEA/Yb-PDI) was tested using Energy Dispersive X-ray Spectroscopy (EDX) as shown in Fig. S13 and S14. The EDX spectrum of the mixed microcrystal shows the uniformly distribution of all four elements at the current resolution, indicating no obviously segregation in the doped microcrystals.

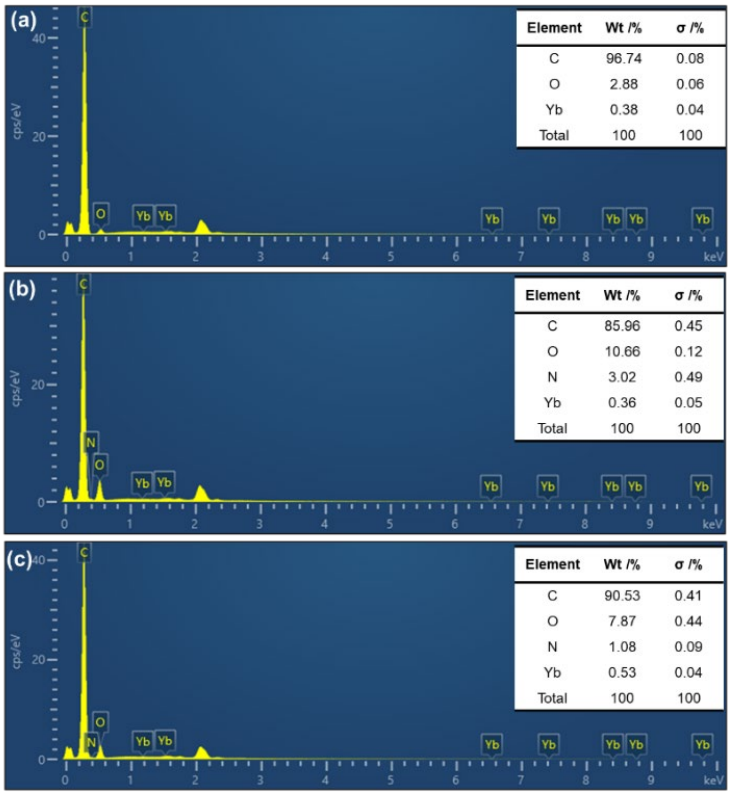

Fig. S14 The EDX spectra of Yb-BPEA (1:30) (a), Yb-PDI (1:10) (b) and mixed TTA-UC microcrystal (Yb-BPEA/Yb-PDI (1:4 w/w)) (c). The insert table is the corresponding elements content.

Supporting Tables

Table S1 Crystal data and structure refinement for $Yb_5(DBM)_{10}(OH)_5$.

Complex	$Yb_5(DBM)_{10}(OH)_5$
Identification code	mx11460_sq
Empirical formula	$C_{150}H_{115}O_{25}Yb_5$
Formula weight	3182.61
Temperature/K	170.00(10)
Crystal system	tetragonal
Space group	P4/n
a/Å	19.0917(2)
b/Å	19.0917(2)
c/Å	18.5086(4)
α/°	90
β/°	90
γ/°	90
Volume/Å^3	6746.3(2)
Z	2
ρ_{calc}g/cm^3	1.567
μ/mm^{-1}	3.501
F(000)	3130.0
Crystal size/mm^3	0.21 × 0.15 × 0.12
Radiation	Mo Kα (λ = 0.71073)
2Θ range for data collection/°	3.734 to 61.95
Index ranges	-24 ≤ h ≤ 23, -24 ≤ k ≤ 26, -22 ≤ l ≤ 26
Reflections collected	53431
Independent reflections	9471 [R_{int} = 0.0336, R_{sigma} = 0.0312]
Data/restraints/parameters	9471/244/475
Goodness-of-fit on F^2	1.058
Final R indexes [I>=2σ (I)]	R_1 = 0.0533, wR_2 = 0.1313
Final R indexes [all data]	R_1 = 0.0884, wR_2 = 0.1563
Largest diff. peak/hole / e Å^{-3}	3.74/-1.42
Identification code	mx11460_sq

Table S2 Fractional Atomic Coordinates (×10^4) and Equivalent Isotropic Displacement Parameters (Å2×10^3) for $Yb_5(DBM)_{10}(OH)_5$. U_{eq} is defined as 1/3 of of the trace of the orthogonalised U_{IJ} tensor

Atom	x	y	z	U(eq)
Yb1	2213.9(2)	3756.7(2)	7010.1(2)	33.84(10)
Yb2	2500	2500	8547.3(3)	43.83(16)
O1	3202(2)	3678(2)	6310(2)	36.6(9)
O2	2898(3)	4681(2)	7368(3)	47.7(11)
O3	1380(3)	4445(3)	7473(3)	51.2(12)
O4	1995(3)	4529(2)	6129(3)	46.4(11)
O6	1672(2)	3035(2)	7801(3)	41.1(10)
O7	2500	2500	6727(5)	30.7(16)
C1	3603(6)	5675(7)	7385(7)	105(4)
C2	3139(10)	6002(10)	7863(10)	165(6)

C3	3280(12)	6682(11)	8120(14)	207(7)
C4	3980(11)	6885(12)	7999(13)	192(7)
C5	4495(10)	6560(8)	7585(9)	145(5)
C6	4257(6)	5963(6)	7233(7)	100(3)
C7	3345(5)	5033(5)	7035(4)	67(3)
C8	3607(4)	4846(4)	6342(4)	52.4(18)
C9	3507(3)	4217(3)	6002(4)	38.2(14)
C10	3714(4)	4117(4)	5231(4)	43.9(15)
C11	4124(4)	4590(4)	4860(5)	57(2)
C12	4258(5)	4507(5)	4131(5)	71(3)
C13	3985(5)	3943(5)	3765(5)	69(2)
C14	3590(5)	3462(5)	4128(4)	62(2)
C15	3450(4)	3541(4)	4855(4)	51.4(17)
C16	1786(4)	5502(4)	5404(6)	63(2)
C17	2172(5)	5201(5)	4871(5)	64(2)
C18	2299(6)	5538(6)	4221(7)	86(3)
C19	2015(6)	6211(7)	4130(8)	102(4)
C20	1632(7)	6524(7)	4658(9)	116(5)
C21	1505(5)	6171(5)	5292(8)	90(4)
C22	1691(4)	5112(4)	6097(5)	50.3(18)
C23	1266(4)	5376(4)	6647(6)	65(2)
C24	1124(4)	5032(4)	7296(6)	59(2)
C25	585(6)	5323(5)	7798(7)	88(3)
C26	365(6)	6018(5)	7751(7)	103(4)
C27	-136(8)	6264(8)	8236(9)	146(5)
C28	-450(10)	5792(8)	8714(11)	167(6)
C29	-252(9)	5090(8)	8774(10)	162(6)
C30	278(8)	4872(7)	8304(8)	129(5)
O5	2602(3)	1484(3)	9173(3)	61.3(14)
C31	405(8)	1997(11)	9581(11)	89(5)
C32	231(12)	2696(12)	9641(13)	109(7)
C33	-459(11)	2841(14)	9814(13)	126(8)
C34	-978(14)	2346(13)	9930(16)	128(8)
C35	-743(12)	1660(15)	9856(15)	140(8)
C36	-67(11)	1458(12)	9683(13)	126(7)
C37	1169(7)	1870(9)	9426(11)	68(4)
C38	1455(7)	1208(9)	9512(11)	72(4)
C39	2153(7)	1043(9)	9397(10)	66(4)
C40	2451(11)	337(10)	9595(12)	96(6)
C41	2101(13)	-66(13)	10106(12)	122(7)
C42	2368(13)	-729(13)	10251(15)	136(8)
C43	2957(13)	-988(16)	9907(14)	138(8)
C44	3302(13)	-580(12)	9397(14)	124(7)
C45	3041(11)	83(12)	9247(13)	113(7)

Table S3 The structures and photophysical parameters of annihilators

Annihilator	structure	Φ_{FL}	E_{T1}/eV	Ref
BPEA	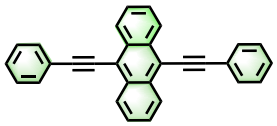	100	1.24-1.36	[6,7]
TIPS	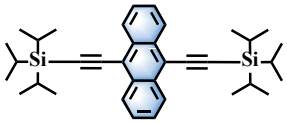	75	1.37	[8,9]
PDI	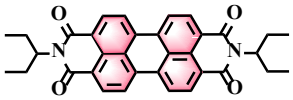	97	1.15	[10]

Reference

1. O. Dolomanov, L. Bourhis, R. Gildea, J. Howard and H. Puschmann, *J. Appl. Cryst. J. Appl. Cryst*, 2009, **42**, 339-341.
2. G. M. Sheldrick, *Acta Crystallogr C Struct Chem*, 2015, **71**, 3-8.
3. H.-Y. Shen, W.-M. Wang, H.-L. Gao and J.-Z. Cui, *RSC Advances*, 2016, **6**, 34165-34174.
4. N. J. R. By L. R. Melby, E. Abramson, and J. C. Caris, *Helv. Chim. Acta*, 1962, **45**.
5. A. Lennartson, M. Vestergren and M. Hakansson, *Chemistry*, 2005, **11**, 1757-1762.
6. Y. J. Bae, G. Kang, C. D. Malliakas, J. N. Nelson, J. Zhou, R. M. Young, Y.-L. Wu, R. P. Van Duyne, G. C. Schatz and M. R. Wasielewski, Journal of the American Chemical Society, 2018, 140, 15140-15144.
7. T.-S. Fang, J. Lin, R. Schneider, T. Yamada and L. A. Singer, Chemical Physics Letters, 1982, 92, 283-287.
8. N. Nishimura, V. Gray, J. R. Allardice, Z. Zhang, A. Pershin, D. Beljonne and A. Rao, ACS Materials Letters, 2019, 1, 660-664.
9. P. Bharmoria, F. Edhborg, H. Bildirir, Y. Sasaki, S. Ghasemi, A. Mårtensson, N. Yanai, N. Kimizuka, B. Albinsson, K. Börjesson and K. Moth-Poulsen, Journal of Materials Chemistry A, 2022, 10, 21279-21290.
10. F. Deng, J. R. Sommer, M. Myahkostupov, K. S. Schanze and F. N. Castellano, Chemical Communications, 2013, 49, 7406-7408.